https://doi.org/10.5194/esurf-2019-59
Preprint. Discussion started: 6 November 2019

Earth Surface Dynamics Discussions
Open Access
EGU

Modelling impacts of spatially variable erosion drivers on suspended sediment dynamics

Giulia Battista[1], Peter Molnar[1], and Paolo Burlando[1]

[1]Institute of Environmental Engineering, ETH Zurich, 8093 Zurich, Switzerland

Correspondence: Giulia Battista (battista@ifu.baug.ethz.ch)

Abstract.

The estimate of suspended sediment load in rivers is often highly problematic because of the strong variability in suspended sediment concentrations with discharge. Previous studies that investigated the sources of this variability highlight the need to explicitly account for the main hydrological processes controlling sediment erosion and transport at the catchment scale, their spatio-temporal variability and interactions with the topography and surface characteristics of the basin. In this paper we propose a novel physically explicit spatially distributed hillslope erosion and sediment transport model including these erosion drivers, based on the computationally efficient hydrological model TOPKAPI-ETH. We investigate its suitability to reproduce the variability of sediment concentrations at the outlet of a pre-alpine river basin in Switzerland and quantify the impacts of key spatially variable erosion drivers - rainfall and surface erodibility - on sediment dynamics. Our analysis shows that deterministic modelling can capture a significant part of the variability in suspended sediment concentrations. Spatial variability of erosion drivers affects sediment yield by (i) increasing sediment production due to a spatially variable precipitation, while decreasing it due to a spatially variable surface erodibility, (ii) favoring the clustering of sediment source areas, and (iii) decreasing their connectivity to the river network by magnifying sediment buffers. Finally, we discuss the results in the context of the geomorphology and landscape characteristics of our study area and compare our findings with other modelling and empirical studies on sources of sediment concentration variability.

1 Introduction

Fine sediment transported in suspension by rivers drives and influences important geomorphic and ecological processes. Human activity strongly interacts with the processes of suspended sediment production and transport, on the one hand by practices which enhance soil erosion, like agriculture, mining and deforestation, and on the other hand with the construction of sediment retention structures like dams (e.g., Syvitski et al., 2005; Montgomery, 2007; Syvitski and Kettner, 2011). The monitoring of suspended sediment concentration is essential to understand how these two opposite disturbances affect the sediment balance. In the context of enhanced soil erosion, phenomena like the loss of soil productivity, the reduction of water quality due to higher turbidity and concentration of pollutants, and accelerated reservoir siltation are expected (e.g. Pimentel et al., 1987; Davies-Colley and Smith, 2001). The combined effect of enhanced soil erosion and sediment retention by dams modifies the river sediment equilibrium and can result in river incision in the case of sediment starvation, undermining the stability of bridges

https://doi.org/10.5194/esurf-2019-59
Preprint. Discussion started: 6 November 2019

Earth Surface Dynamics Discussions
Open Access
EGU

and other infrastructures, and eventually in coastal erosion, leading to increased flood risk in coastal areas (Chen and Zong, 1998; Schmidt and Wilcock, 2008). The opposite case of excessive sediment load in rivers may also lead to an increase in flood risk in alluvial floodplains due to sediment deposition (Walling, 2006; Rickenmann et al., 2016). The intensity of these effects is expected to grow in the future, as the magnitude and number of highly erosive extreme precipitation events are expected to increase due to climate change (e.g. Nearing et al., 2004; Yang et al., 2003).

The most widespread method for sediment yield estimation from intermittent measurements of sediment concentration are sediment-discharge rating curves (see Gao (2008) for a review). However, the development of these curves is often highly problematic because of the strong non-uniqueness of suspended sediment concentrations (SSCs). The same value of discharge (Q) often leads to a wide range of SSCs, producing highly scattered SSC-Q rating curves (e.g., Walling, 1977; Ferguson, 1986; Asselman, 2000; Walling and Webb, 1982; Horowitz, 2003). The strong variability in SSC is attributed to the high non-linearity of the sediment production and transport processes in time and space, and the presence of threshold and feedback mechanisms in sediment mobilization (e.g., Fryirs et al., 2007; Bracken et al., 2015; Asselman, 1999; Seeger et al., 2004; Collins and Walling, 2004).

Drivers of temporal variability in sediment transport are identified in the dynamic nature of meteorological forcing and hydrological conditions, in the differential activation of the dominant sediment sources, and in natural or artificial modifications of hillslope and channel sediment connectivity (e.g. Vercruysse et al., 2017). Geomorphic internal variability may also play a role as a driver of temporal variability of soil loss at the plot scale (Kim et al., 2016). Spatial variability in sediment transport is driven by the distribution of sediment sources within the catchment and the transport capacity of the erosive agents, catchment connectivity and efficiency of sediment transport within the stream network (e.g. Vercruysse et al., 2017).

It is not simple to identify the different sources of variability in sediment production. Some studies have investigated the relationship between hydrometeorological conditions and suspended sediment transport, where a particular focus has been on the shape and direction of the hysteresis loops of the SSC-Q relation (Dominic et al., 2015; Seeger et al., 2004; Duvert et al., 2010; Zabaleta et al., 2007; Smith et al., 2003). The effects of human landscape modifications on the SSCs have also been explored, for example by looking at the consequences of land use change and flow regulation (Siakeu et al., 2004; Olarieta et al., 1999; Costa et al., 2018). A few studies focused on the spatial distribution of catchment characteristics and erosion drivers at the river basin scale. Among those, Wass and Leeks (1999) related differences in sediment loads across the basin to geomorphic and climatic gradients. Some studies reconstructed the change in time of sediment sources on hillslopes and their coupling with the channels (Fryirs and Brierley, 1999; Lang et al., 2003) and developed conceptual frameworks for sediment connectivity at multiple spatial and temporal scales (Fryirs, 2013; Bracken et al., 2015).

The above studies highlight the need to account for both types of variability (time and space) in order to investigate sediment dynamics. Therefore, when modelling suspended sediment transport at the catchment scale it is necessary to explicitly account for the main hydrological processes, their temporal dynamics and distribution in space, as well as their interaction with the topography and morphology of the basin. Moreover, there is a need for these models to be suitable for medium to large scale catchment applications, where the gradients of climatic and physiographic variables are more relevant. Such models are then

https://doi.org/10.5194/esurf-2019-59
Preprint. Discussion started: 6 November 2019


Earth Surface Dynamics Discussions
Open Access
EGU

expected to reproduce the spatio-temporal variability of suspended sediment concentrations and to serve as a tool to investigate its causes.

Several existing distributed soil erosion sediment transport models are partially suitable for this task. However, most of them are only suitable for event-applications (Answers (Beasley et al., 1980), KINEROS (Woolhiser et al., 1990), WEPP (Nearing et al., 1989)) or present highly simplified, if not absent, hydrological components, as in the case of WATEM/SEDEM (Van Rompaey et al., 2001) or landscape evolution models, e.g. Cesar-Lisflood (Coulthard et al., 2013), SIBERIA (Hancock et al., 2000). More suitable approaches are tRIBS (Francipane et al., 2012), which includes a physically based long-term hydrological component, however it is only suitable for small scale applications. On the other end of the spectrum, Tsuruta et al. (2018) developed a spatially distributed model especially for large basins, which being based on a land-surface model, presents an approximated coarse-scale representation of hydrological and sediment connectivity on the hillslopes.

In this work, we propose a novel spatially distributed hillslope erosion and sediment transport model, obtained by integrating a sediment production and transport component within the computationally efficient physically explicit hydrological model TOPKAPI-ETH (Fatichi et al., 2015). This hydrological model contains a physically meaningful representation of hydrological processes and is at the same time suitable for large scale, high resolution and long term simulations. We present the application of the model to a medium-size pre-alpine river basin and we investigate its suitability to reproduce variability in sediment transport. We focus specifically on the impact of spatially variable erosion drivers - rainfall and surface erodibilty - on suspended sediment dynamics at the catchment scale. We aim at addressing the following research questions: (RQ 1) To which extent can a physically explicit spatially distributed deterministic model capture the variability of suspended sediment concentrations? (RQ 2) How does the spatial variability of key erosion drivers affect the spatial organization of suspended sediment transport, i.e. the location and productivity of sediment sources and their connectivity to the river network? (RQ 3) How does sediment yield at the outlet depend on the spatial organization of suspended sediment transport?

2 Methods

The Kleine Emme river basin is a glacier-free pre-alpine catchment located in central Switzerland. It has an area of 477 km^2, an elevation range of 430-2300 m. a.s.l. and a mean annual precipitation of 1650 mm (Figure 1a). The average discharge at the outlet is 12.6 m^3/s. The catchment is mostly natural, with more than 50% of the catchment surface covered by forest and grassland (Figure 1c). The Kleine Emme was chosen as a study basin because the natural regime of water and sediment flow is almost unaltered. No use of water for irrigation or hydropower is known and sediment-retaining infrastructures are absent. Moreover, the absence of glaciers means that fine sediment production in the basin is mostly driven by overland flow. Finally, the diverse geomorphology of the basin has been subject of several studies and long-term estimates of denudation rates are available (e.g., Schwab et al., 2008; Dürst Stucki et al., 2012; Schlunegger and Schneider, 2005; Van Den Berg et al., 2012; Clapuyt et al., 2019).

Measurements of precipitation, air temperature and sunshine radiation are available from automatic weather stations located inside or in the vicinity of the basin operated by MeteoSwiss. The information about the spatial distribution of precipitation

https://doi.org/10.5194/esurf-2019-59
Preprint. Discussion started: 6 November 2019

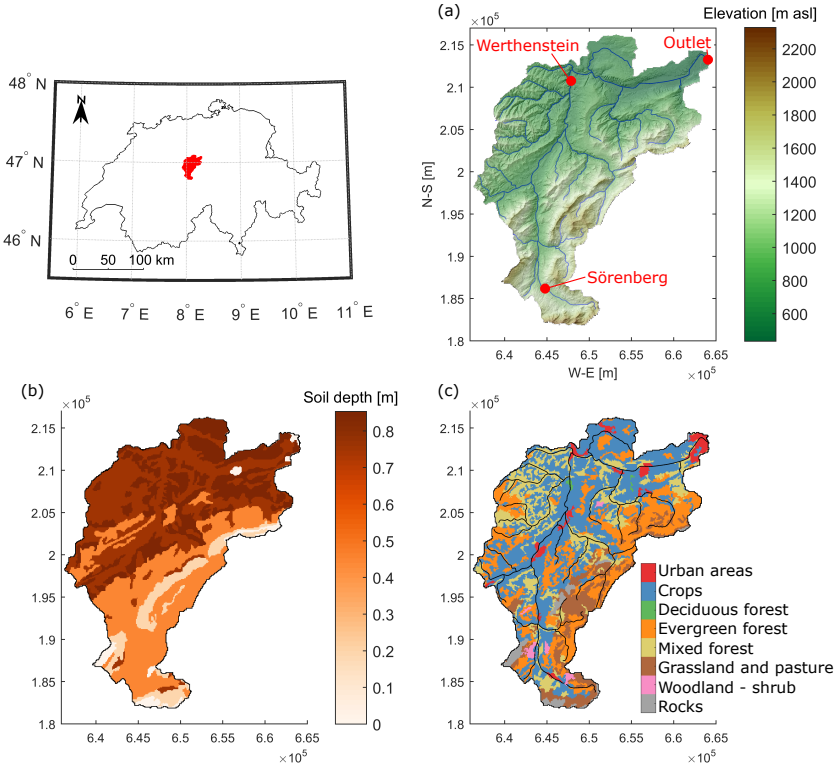

Figure 1. (a) Digital Elevation Model (DEM) of the Kleine Emme basin and location of discharge gauges (source SwissAlti3D, 2017), (b) Soil depth, derived from the Swiss soil map (Bodeneignungskarte, 2012), (c) Land cover derived from Corine Land Cover map (CLC, 2014).

inside the basin area is available from the 1x1 km daily gridded product of MeteoSwiss RhiresD (Frei and Schär, 1998; Schwarb, 2000). Streamflow is monitored at Werthenstein and at the basin outlet by the Federal Office of the Environment and at Sörenberg by the Canton Luzern (Figure 1). SSCs have been manually sampled at the outlet since 1974, but with a regular frequency of two samples a week only since 2004. The information about soil type and depth for the basin is available from the soil map of Switzerland (Bodeneignungskarte, 2012) (Figure 1b). Land cover is provided by the Corine Land Cover (Figure 1c).

2.1 Hydrology-sediment model description

The model we present in this work is an extension of the hydrological model TOPKAPI-ETH (Fatichi et al., 2015), which we integrated with a new hillslope erosion and channel suspended sediment flow module. The TOPKAPI-ETH hydrological model was chosen because of its spatially distributed nature and physically explicit representation of the major hydrological processes. In TOPKAPI-ETH 2D surface and subsurface flow is simulated by the kinematic wave approximation, with resistance to flow given by surface roughness and soil transmissivity as a function of soil properties. Water may saturate the soil and lead to

https://doi.org/10.5194/esurf-2019-59
Preprint. Discussion started: 6 November 2019

overland flow generation by saturation excess or by infiltration excess in case of high rainfall intensities. Soil is dried by evapotransporation and drainage and the model includes snow cover accumulation and melt, which are important in the water balance of Alpine basins (see Fatichi et al., 2015). Moreover, the model is particularly suitable for catchment scale, long-term, high resolution simulations (hourly time step, grid resolution ~100 m), even when integrated with a sediment production and transport component, since the kinematic wave approximation of the surface and subsurface flow routing are solved analytically and thus keep the model computationally efficient (Liu and Todini, 2002).

In the newly developed sediment module of TOPKAPI-ETH, the generation of fine sediment is assumed to take place on the hillslopes by the erosive action of overland flow. The eroded sediment is routed downstream via overland flow, which is assumed to transport at its maximum capacity and can deposit or erode at a rate D depending on the hydraulic and topographic properties of the cells along the flow path:

$$D = \nabla \cdot q_s, \tag{1}$$

where q_s is the overland flow transport capacity, modelled following Prosser and Rustomji (2000) as a function of specific overland flow discharge q and the surface slope S:

$$q_s = \alpha q^{\beta} S^{\gamma}, \tag{2}$$

where β and γ are transport exponents, and α is a calibration parameter that captures the effect of land surface and soil properties on erosion and sediment transport.

The suspended sediment flux in the river network is treated as an advection process and solved with the same numerical methods used for water flow. The equation of suspended sediment flux in the channel is:

$$\frac{\partial AC}{\partial t} = E - \frac{\partial QC}{\partial x}, \tag{3}$$

where Q is the river discharge, C is the SSC, A is the cross-section area of flow and E is the term representing the exchange of sediment with the bed and local sediment sources. By following the reasoning of Liu and Todini (2002), eq. 3 can be integrated over a grid cell, within which the values of the variables are assumed to be constant, and then solved analytically as a first-order ordinary differential equation:

$$\frac{\partial V_i C_i}{\partial t} = E_i X + Q_{in} C_{in} - \frac{U_i}{X} C_i V_i, \tag{4}$$

where X is the grid cell size, V_i the volume of water inside a cell ($V_i = A_i X_i$), U_i the mean flow velocity, C_i and E_i are the mean values of C and E inside the grid-cell. Q_{in} and C_{in} are the discharge and sediment concentration entering the cell i from the upstream grid-cell $(i-1)$.

2.2 Model setup and calibration

2.2.1 Hydrology

Given the period of availability of suspended sediment measurements, the simulation was set up for the years 2003 to 2016, where the first year is considered a warm-up period. The meteorological input data required by the hydrological component of

https://doi.org/10.5194/esurf-2019-59
Preprint. Discussion started: 6 November 2019

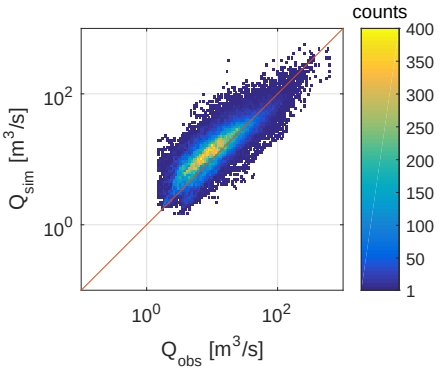

Figure 2. Density plot of observed vs simulated hourly discharges at the outlet for the period 2004-2016.

TOPKAPI-ETH are hourly precipitation, air temperature and cloud cover. The precipitation input file was created by combining station and gridded precipitation datasets following the approach of Paschalis et al. (2014). In this approach hourly precipitation measured at the rain gauges was spatially interpolated to match the spatial distribution of the daily precipitation reported by the gridded RhiresD dataset. The hourly time series of measured air temperature were extrapolated across the model domain to different elevations with a temperature lapse rate of of 5.5 °C/km. The cloud cover transmissivity was derived from the hourly sunshine duration measurements following the empirical relation proposed by Kasten and Czeplak (1980).

The model was run at a 100x100 m^2 spatial resolution and a constant time step of 1-hour. To initiate the model calibration, realistic values of the hydrological parameters were assigned based on the soil characteristics and previous investigations (Paschalis et al., 2014; Pappas et al., 2015). The soil hydraulic conductivity and the residual and saturation soil water content parameters were then adjusted in order to maximize the performance of the hydrological model in terms of correlation coefficient and Nash-Sutcliffe efficiency (NSE) for runoff measured at three streamflow gauging stations.

The final configuration of the hydrological model performed very well in reproducing the observed discharge at the outlet and at Werthenstein (see Table 1 and Figure 2). Discharge data are available at a sub-daily resolution at Sörenberg only from the year 2005, therefore the evaluation of the performance at this station does not consider the first year of simulation. The model performance at this station is slightly worse, probably due to the lower accuracy of the measurements, but still satisfactory.

2.2.2 Setup of the sediment module

The inputs needed to run the hillslope erosion and suspended sediment transport modules are the parameters α, β and γ in eq. 2 and parameter E in eq. 3. The β and γ parameters are assumed spatially uniform and equal to 1.4, following Prosser and Rustomji (2000). The parameter α contains information about the soil and land surface properties that influence the rate of soil erosion. We derived the spatial distribution of α by intersecting the soil erodibility parameter K of the Universal Soil Loss equation (USLE), computed for Switzerland by Schmidt et al. (2018), and the land use USLE parameter C, which we derived from Yang et al. (2003) (see Figure S1). In this way we implicitly account for the influence of particle size distribution, organic

https://doi.org/10.5194/esurf-2019-59
Preprint. Discussion started: 6 November 2019

Earth Surface Dynamics Discussions
Open Access
EGU

Table 1. Hydrological performance for the simulation period 2004-2016 at the three flow monitoring stations in terms of correlation coefficient (r), Nash-Sutcliffe efficiency (NSE) and root mean square error (RMSE).

	Outlet			Werthenstein			Sörenberg (2005-16)		
	r	NSE	RMSE $[m^3/s]$	r	NSE	RMSE $[m^3/s]$	r	NSE	RMSE $[m^3/s]$
Hour	0.84	0.69	0.75	0.84	0.65	0.74	0.63	0.72	1.43
Day	0.91	0.80	0.53	0.90	0.78	0.52	0.80	0.56	0.83
Month	0.93	0.76	0.28	0.92	0.77	0.26	0.88	0.77	0.38
Year	0.93	-	0.18	0.92	-	0.13	0.79	-	0.10

matter content, soil structure, permeability, surface roughness and vegetation cover in determining the spatial distribution of surface erodibility. A comparable approach is proposed by Hancock et al. (2017).

The ratio between the product of C and K of the different classes was then kept constant in the calibration process and α was calibrated by multiplying the CK values by a spatially constant parameter α_1:

$$\alpha(x,y) = \alpha_1 C(x,y) K(x,y), \tag{5}$$

where x and y are coordinates in space. With respect to the channel processes, the time resolution of the suspended sediment measurements at the outlet is not sufficient to quantify the exchange of suspended sediment between the water column and the river bed and the contribution of localized channel sources. For this reason, in this work the term E in equation 3 has been assumed equal to zero. The absence of fine sediment exchange with the bed is a reasonable assumption for this case study, as significant deposits of fine sediment are not present in the river bed and bedrock is often exposed, indicating an efficient fine sediment transport downstream (Schwab et al., 2008). Neglecting localized channel sources is instead an approximation of the sediment production processes of the basin. Also on the hillslopes, localized sediment sources are not explicitly modelled and are present only insofar they are represented by high C and K values. The lack of explicit inclusion of point sediment sources and their modelling is a limitation of the current model, which we will address in future work.

2.2.3 Calibration of the sediment module

We found that the parameters that have the highest influence on matching the observed SSC at the outlet are the extension of the modelled river network, dependent on the river initiation threshold, RT, and the α_1 constant. RT defines the upstream area below which water flow is described as overland flow and above which it is described as channelized flow in TOPKAPI-ETH. This parameter has a small influence on discharge, as shown by Table S1, while it is a relevant parameter for the modelling of hillslope erosion and sediment transport. Since fine sediment production can only take place on the hillslopes, the extension

https://doi.org/10.5194/esurf-2019-59
Preprint. Discussion started: 6 November 2019

Earth Surface Dynamics Discussions
Open Access
EGU

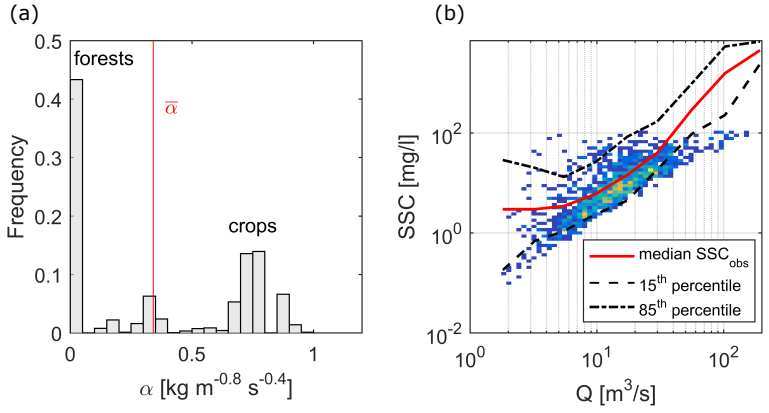

Figure 3. (a) Frequency distribution of the calibrated surface erodibility parameter α, (b) density plot of the simulated SSC at outlet compared with measurements, the lines show the median (red) and 15^{th} and 85^{th} percentile (dashed) of the observations.

of the channels onto the hillslopes influences the magnitude of the sediment input into first-order channels and subsequently downstream through the river network.

The best combination of the calibration parameters was chosen by minimizing the errors between the measured and modelled slope of the SSC-Q cloud of points and the mean and variance of the observed SSCs. The final calibrated parameters were α_1=0.0138 kg m$^{2.2}$ s$^{-3.4}$ and RT=0.4 km^2. The resulting spatial mean of α is $0.3412\ kg\ m^{-0.8}s^{-0.4}$. The histogram of α and its spatial distribution are shown in Figures 3a and 6d, respectively. We note that the calibrated river initiation threshold is very close to the drainage area that Schlunegger and Schneider (2005) propose as the threshold area at which channelized processes become dominant on hillslope processes in the development of the landscape in this study basin (0.1-0.2 km^2).

Using this parameterization, the slope of the measured SSC-Q cloud of points is captured very well for moderate discharges (Figure 3b), whereas the model underestimates the concentrations at highest discharges. If we limit the observed SSC dataset at its 85^{th} percentile and compare it with the simulated concentrations sampled at the hours of collection of the suspended sediment bottle samples, the model reproduces the mean and variance of the observed concentrations with very small errors ($\overline{SSC}_{sim} = 12.40\ mg/l$, $\overline{SSC}_{obs} = 12.20\ mg/l$; $\sigma^2_{sim} = 210.47\ mg/l$,$\sigma^2_{obs} = 233.15\ mg/l$) (Figure S2). We attribute the underestimation of high sediment concentrations (above 85^{th} percentile) to the simplified representation of the sediment production processes in the model and in particular to the lack of point sediment sources like landslides, debris flows and bank erosion.

2.3 Simulation experiments

In order to investigate the causal processes explaining the scatter in the SSC-Q relation and how they affect the spatial organization of sediment transport, we performed simulation experiments which quantify the role of spatial variability in erosion drivers - precipitation and surface erodibility. Precipitation is the main hydrological driver of hillslope erosion through the overland flow term q^β in eq. 2. Surface erodibility is represented by the parameter α in eq. 2.

https://doi.org/10.5194/esurf-2019-59
Preprint. Discussion started: 6 November 2019

Earth Surface Dynamics Discussions
Open Access
EGU

We designed four numerical experiments by combining spatially variable and/or uniform distributions of the two erosion drivers (Figure 4). The reference experiment (SIM 1) accounts for the highest level of complexity by considering both precipitation and erodibility variable in space. This is the experiment with which the model was calibrated. The second experiment (SIM 2) aims to quantify the role of the spatial variability in precipitation, by reducing it to be uniformly distributed in space. The temporal variability was preserved by setting the hourly precipitation in each cell equal to the mean hourly distributed precipitation over the catchment. The third experiment (SIM 3) is designed to investigate the role of the spatial variability in surface erodibility by reducing it to uniform surface erodibility throughout the basin equal to the mean value of the calibrated spatial distribution of α. We completed the set of simulations by performing a fourth experiment (SIM 4) where the spatial variability in both drivers was reduced to uniform precipitation distribution and uniform surface erodibility, to quantify the combined effect of the two erosion drivers.

3 Results

In this chapter, in section 3.1 we evaluate spatio-temporal variability in sediment production and transport and the scatter of the SSC-Q relation it produces by the fully distributed erosion drivers in SIM 1 (RQ 1). The spatial organization of suspended sediment transport is then evaluated in subsequent sections (RQ 2). Here we compare the activation of sediment sources and the sediment production in the four simulations (section 3.2) and we quantify the connectivity of sediment transport by means of the sediment delivery ratio (section 3.3). Finally, in section 3.4, we analyze how the spatial organization of suspended sediment transport affects the sediment loads in the four simulations (RQ 3).

3.1 Spatio-temporal variability in erosion and sediment transport

Figure 3 shows that, with the exception of the highest and lowest discharges, the modelled scatter in the SSC-Q relation compares well with the variability of the measured concentrations (explaining about 30% of the measured concentration range for discharges up to the 85^{th} percentile). In the following we analyse the sources of this variability, by showing the time series of discharge, sediment load and concentration for one representative year (Figure 5a) and analysing the pattern of erosion and deposition across the basin from the entire simulation period (Figure 5b).

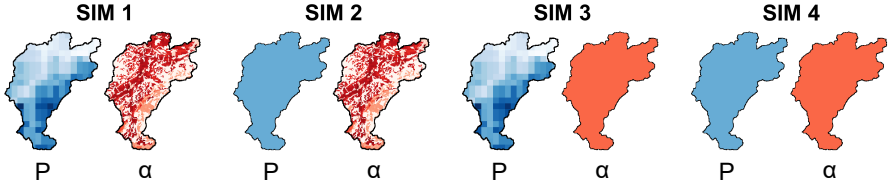

Figure 4. Summary of model runs: in SIM 1 sediment production and transport are driven by a spatially distributed precipitation (P) and surface erodibility (α), in SIM 2 and SIM 3 the spatial variability in precipitation and surface erodibility have been removed, respectively, and in SIM 4 both spatial variabilities have been removed.

https://doi.org/10.5194/esurf-2019-59
Preprint. Discussion started: 6 November 2019

Earth Surface Dynamics Discussions
Open Access
EGU

High sediment fluxes in April and May indicate the contribution of snowmelt to discharge and the erosion of the surface by widespread overland flow. Summer events (storms) provide a small contribution to the yearly sediment yield, however, they generate some of the highest sediment concentrations even though the runoff remains low. In winter months, snow covers the majority of the catchment and maintains the sediment flux very close to zero (Figure 5a).

Most of the erosion is simulated in the south-eastern part of the basin, where slopes are steeper, soil is thinner and the highest precipitation, snow accumulation and melt occur. In these regions, it is easier to saturate the soil layer and generate runoff over larger areas that merge and generate sheets of overland flow, thus producing wide erosional areas on steep mountain flanks. Deposition is simulated at the valley bottoms or at locations of slope reduction. In the north-western part of the basin, overland flow remains constrained to the channel headwaters due to the deeper soil and to the higher drainage density of the area. We observe that because of the transport capacity approach applied in the hillslope transport module, areas of strong erosion often come associated with significant deposition downstream. In the following, we will refer to these areas as sediment source areas.

The mean annual sediment load generated by SIM 1 is $1.42\ 10^4\ t/y$, which is an underestimation of the $2.83\ 10^5\ t/y$ computed from the measurements at Littau by Hinderer et al. (2013). Consistently, the mean annual erosion rate of $0.07\ mm/y$ underestimates the denudation rates derived from ^{10}Be samples in the Entlen and Fontanne by Van Den Berg et al. (2012), Wittmann et al. (2007) and Norton et al. (2008) (between 0.38 and 0.52 mm/y), which are from active erosion areas and integrate over a much longer time span of about 10^4 years. The underestimation of sediment load and erosion rates by our model compared to such data is expected and is attributable to fact that we do not aim to reproduce the largest measured sediment concentrations. This limitation will be further discussed in section 4.1.

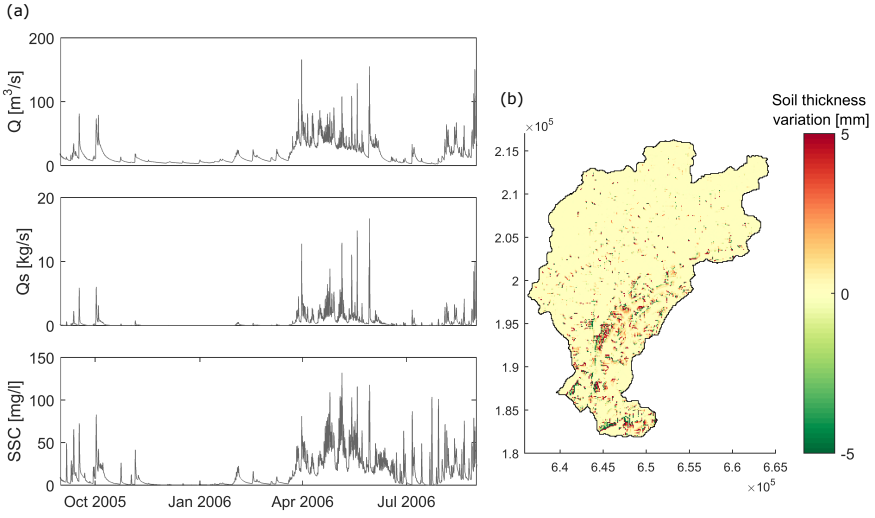

Figure 5. (a) Time series of hourly modelled discharge, suspended sediment load and concentrations for one year at the outlet, (b) change in soil thickness at the end of the 13-year simulation. Positive values indicate erosion, negative values indicate deposition.

https://doi.org/10.5194/esurf-2019-59
Preprint. Discussion started: 6 November 2019

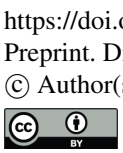

Earth Surface Dynamics Discussions
Open Access
EGU

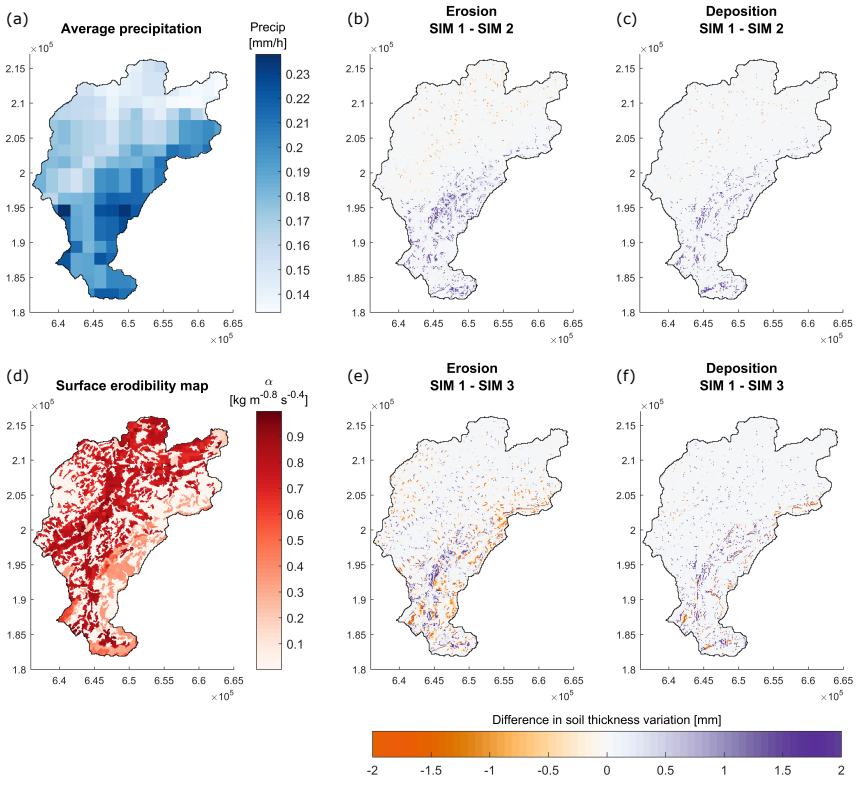

Figure 6. (a) Average spatial distribution of precipitation for the period 2003-2016, (b,c) difference between erosion/deposition generated by distributed and uniform rainfall in 13 years, (d) spatial distribution of calibrated surface erodibility α, (e,f) difference between erosion/deposition generated by distributed and uniform surface erodibility in 13 years. A positive value indicates that distributed precipitation or surface erodibility determines more erosion/less deposition than uniform precipitation or surface erodibility.

3.2 Sediment sources and sediment production

The effect of the spatial variability in precipitation and surface erodibility on the distribution of sediment source areas is shown in Figure 6, where SIM 1, 2 and 3 are compared. Figures 6b and 6c show the difference between the variable and uniform precipitation maps for erosion and deposition, respectively. Similarly, Figures 6e and 6f show the difference between the variable and uniform surface erodibility maps for erosion and deposition separately.

The results show that with uniform precipitation, erosion and deposition are reduced in the south-eastern part of the basin and increased in the north-western. The overall patterns reflect the average spatial distribution of precipitation in the Kleine Emme catchment for the years 2003-2016, with the highest mean rain intensities associated with more erosion (Figure 6a). Uniform surface erodibility increases sediment erosion and deposition in the forested areas and reduces them in crops. In both cases, the overall effect of removing the spatial variability in erosion drivers is a more uniform distribution of the sediment source areas across the basin.

https://doi.org/10.5194/esurf-2019-59
Preprint. Discussion started: 6 November 2019

Earth Surface Dynamics Discussions
Open Access
EGU

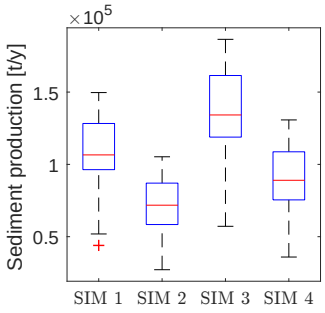

Figure 7. Sediment production in the basin as total sediment detached over a year. Boxplots (median, interquartile range and outliers) show the internal variability in the period 2004-2016.

To quantify the erosional power of the four combinations of erosion drivers, we computed the total sediment mass detached yearly across the whole basin (referred to as sediment production) in the four simulations. The distribution of the yearly sediment production with interannual variability is reported in Figure 7. We observe that the removal of spatial variability generates two opposite effects for precipitation and surface erodibility. Sediment production increases when removing the spatial variability in surface erodibility and decreases when removing the spatial variability in precipitation. In SIM 4 the balance between the two opposing effects determines a slight overall reduction in sediment production. The differences between the scenarios are within natural interannual variability in sediment production, but they are all statistically significant for change in median.

3.3 Connectivity of sediment transport

The connectivity of sediment transport, i.e sediment source areas linked to the river network, within the catchment for the different simulation configurations has been quantified by means of the sediment delivery ratio (SDR). The SDR is defined according to Walling (1983) as the ratio of the sediment delivered at the outlet of a selected area to the gross erosion in that area. The mean annual SDRs, which were computed at the outlet point of the main tributaries and at several cross-sections along the main channel, are reported in Figure 8 as a function of the drainage area.

Sediment connectivity along the main channel shows an increasing trend as a function of the upstream area for both SIM 1 and SIM 3 (Figure 8b). This trend is explained by the higher SDR of the tributaries compared to that of the main channel and by the absence of significant sediment sinks in the main channel. For the subbasins with outlets along the main channel, removing the spatial variability in surface erodibility (SIM 3) has the overall effect to increase sediment connectivity. In some tributaries, however, the opposite effect is observed (T5 and T6). Figure 8c compares the sediment connectivity in the four simulations in the main channel SDR. It shows that removing the spatial variability in precipitation (SIM 2 and 4) also increases the SDR, therefore sediment connectivity (compared to SIM 1 and 3, respectively).

https://doi.org/10.5194/esurf-2019-59
Preprint. Discussion started: 6 November 2019

Earth Surface Dynamics Discussions
Open Access
EGU

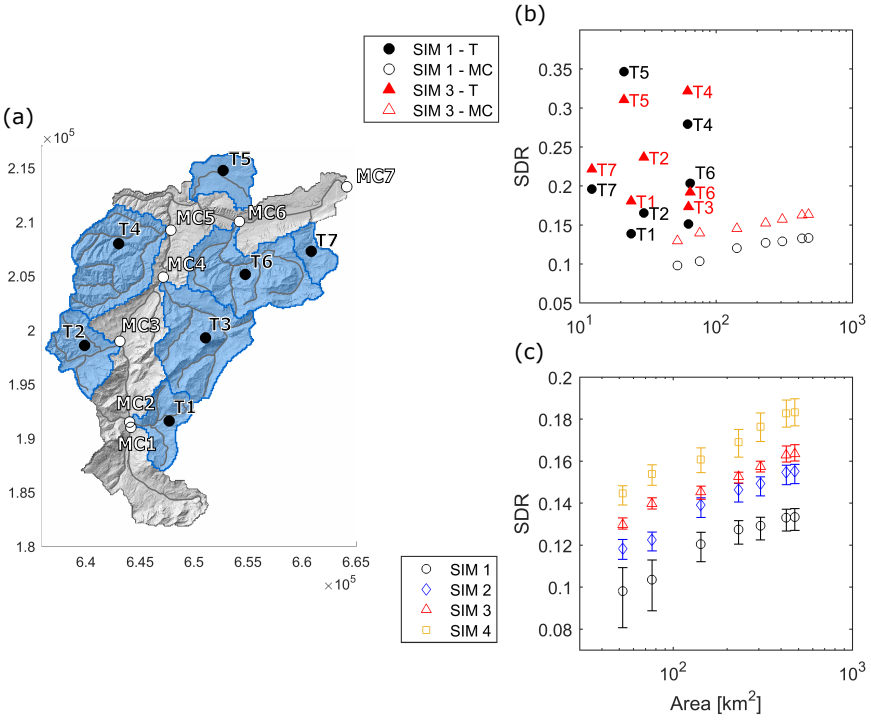

Figure 8. (a) Locations where the sediment delivery ratio has been computed: in main tributaries (T) and along the main channel (MC) in the Kleine Emme basin, (b) mean annual SDR vs drainage area for tributaries and points along the main channel for distributed rainfall simulations, (c) comparison of mean annual SDRs for main channel points for the four simulations. The error bars show the interquartile range of the annual SDR variability.

3.4 Sediment loads and initial soil moisture

The distribution of annual sediment yields at the outlet generated by the four simulation experiments shows that distributed precipitation simulations (SIM 1 and 3) generate higher sediment loads than their uniform precipitation equivalents (SIM 2 and 4) (Figure 9a). Distributed erodibility (SIM 1 and 2) produces smaller sediment loads than uniform erodibility (SIM 3 and 4). To further investigate the differences among the sediment yield distributions, in Figure 9b we show the influence of spatial variability in rainfall and surface erodibility on event-based sediment yields for high and low initial soil moisture (SM_0) conditions. After separating the outlet hydrograph into single events, we computed the total sediment yields for each event and compared the distributions of the events with high and low initial soil moisture. Low SM_0 events are defined as those with SM_0 smaller than the 20^{th} percentile of the SM_0 distribution; high SM_0 events have a SM_0 greater than the 80^{th} percentile.

Although the distributions of event sediment yields largely overlap, we observe that, as expected, the distribution of event yields is more affected by the precipitation spatial variability when the SM_0 is low. The differences between the median, 25^{th}

https://doi.org/10.5194/esurf-2019-59
Preprint. Discussion started: 6 November 2019

Earth Surface Dynamics Discussions
Open Access
EGU

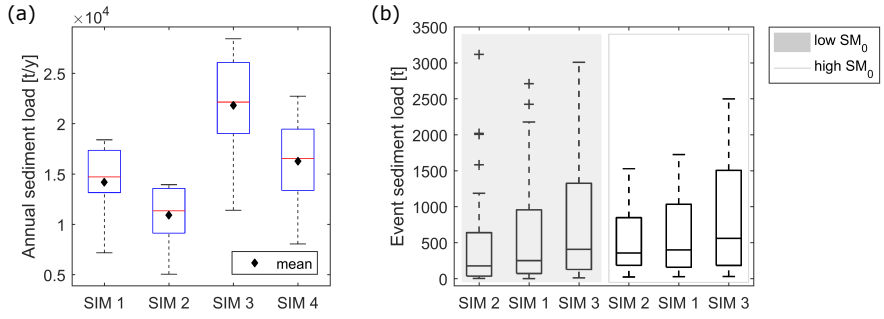

Figure 9. (a) Boxplots of annual sediment load and their mean values in the four simulation experiments, (b) boxplots of event sediment loads divided into low and high initial soil moisture conditions. The boxplots compare the effect of the spatial variability in precipitation and surface erodibility on events with different initial soil moisture.

and 75^{th} percentile of the SIM 1 and 2 are bigger for low SM_0 than for high SM_0. On the contrary, removing variability in surface erodibility seems to equally affect low and high initial SM_0 events.

4 Discussion

4.1 Sources of concentration variability

The modelling approach presented here reproduces a significant part of the observed SSC-Q relation scatter, thus implying that it contains important sources of sediment concentration variability in time and space at the catchment scale. These sources are identifiable in the time-varying meteorological inputs and in the spatially distributed nature of the model and are present even in deterministic modelling of the hydrology and sediment transport.

The precipitation input combines both temporal and spatial components of variability. The temporal component is visible in Figure 5, showing that the same sediment concentration can correspond to a large range of discharge values, depending on the type of event and initial conditions that produce it. Spatial variability in precipitation contributes to the SSC-Q scatter, by allowing the same discharge at the outlet to be generated by many combinations of overland flow situations over the hillslopes. Each of these combinations activates different sediment sources that have a characteristic hydrological and sediment signal and connectivity to the river network. In particular, we identify localized high-intensity summer storms as a main source of scatter, while snowmelt and winter storms produce a more homogeneous response throughout the basin. The spatially variable surface erodibility can additionally contribute to the uniqueness of the sediment signals of the activated source areas, when its spatial distribution is such to enhance the topographic heterogeneity within the basin.

Other sources of variability in sediment transport are implicit in the spatially distributed nature of the model, which allows to account for the heterogeneity of topography, soil depth and soil properties. These heterogeneities are responsible for the residual scatter of SIM 4, where the variability of both erosion drivers have been removed.

https://doi.org/10.5194/esurf-2019-59
Preprint. Discussion started: 6 November 2019

Because the sediment storage on hillslope cells is not exhausted during our simulation experiments, sediment availability does not influence sediment production in our study. Therefore, sediment availability in our simulation experiments does not drive changes in the dominant sediment sources and does not add spatial variability to the sediment response.

The main limitation of our approach in reproducing SSC variability is the lack of processes representing very localized sediment sources, which are usually characterized by a threshold behavior and therefore diversify the local sediment response. In this respect, Schwab et al. (2008) showed that in the Kleine Emme basin short time scale threshold processes are responsible for the export of regolith produced by soil creep in landslides. The absence of these processes in our model could justify not only the smaller-than-observed modelled scatter, but also the underestimation of the highest SSCs, of the soil erosion rate and annual sediment load, observed in section 3.1. Finally, we acknowledge that also inherent stochasticity in the sediment production and transport might explain part of the observed SSC-Q rating curve scatter (Malmon et al., 2003; Fuller et al., 2003). We are working on overcoming these model limitations in the future.

4.2 Spatial organization of suspended sediment transport

The explicit combination of hydrological processes and topographic and land use effects in the model allows to investigate how the spatial variability in erosion drivers affects the spatial organization of sediment transport. Spatial variability enhances the heterogeneity of erosion and deposition across the catchment, thus favoring the clustering of sediment source areas. Sediment production is increased by the spatial aggregation of precipitation (SIM 1 and SIM 3), due to increased erosive power. The effect of a spatially variabile surface erodibility depends on the distribution of overland flow relative to that of surface erodibility and, in this case, the lower sediment productions of SIM 1 and 2 indicate that the two distributions combine more intense overland flow with lower erodibility areas, thus reducing the overall sediment production.

As shown by the sediment delivery ratio, the connectivity of sediment sources is reduced by the spatial variability of precipitation and this effect can be explained by the geomorphic connectivity of the catchment. The concentration of the distributed precipitation, the shallower soils and steeper slopes in the southeastern region of the basin, i.e. tributaries T1, T3, T6 and the upper stretch of the main channel, favor overland flow generation, and thus hydrological connectivity. However, the lower topographic connectivity of these subbasins overall determines a reduction in the sediment transport connectivity. Such lower connectivity is indicated by the low SDRs of these subbasins in SIM 3, which does not account for the land use effect, and suggests the presence of geomorphic sediment buffers (Fryirs, 2013). The different topographic connectivity of the southeastern and northwestern regions reflects the different geomorphology of the two parts of the basin. In fact, the southeastern region of the basin is characterized by a predominantly Last Glacial Maximum landscape with wide valleys and major instabilities, which are in most cases not directly connected to the river network (Van Den Berg et al., 2012; Schwab et al., 2008; Clapuyt et al., 2019). On the other hand, the northwestern part of the basin, i.e. tributaries T4 and T5, shows a rejuvenating landscape where recent fluvial dissection created narrow and deeply incised valleys with a strong coupling between hillslopes and channels (Norton et al., 2008; Schlunegger and Schneider, 2005).

The reduction of sediment transport connectivity by spatially distributed surface erodibility can be attributed to the hypothesis applied in the sediment module that sediment discharge is always in equilibrium with the overland flow transport capacity.

https://doi.org/10.5194/esurf-2019-59
Preprint. Discussion started: 6 November 2019

Based on this assumption, a spatially variable α allows, on the one hand to modulate the sediment production in space and, on the other hand, to define preferential areas of sediment deposition and therefore to define sediment connectivity. By associating a lower transport capacity to forests, their role as sediment buffers blocking sediments will emerge. Vice versa, high α values in grasslands will mean the absence of obstacles to sediment flux. Therefore, the smaller sediment transport connectivity of SIM 1 and 2 compared to SIM 3 and 4 reflects the location of sediment buffers (i.e. forests) with respect to the channel network. In fact, in most of the basin, forested areas surround channel headwaters, thus disconnecting the sediment sources on the hillslopes and mountain flanks to enter the river network (see also, Clinnick, 1985; Schoonover et al., 2006; Parkyn et al., 2005; Mekonnen et al., 2015).

4.3 Sediment load and connectivity

The analyses presented in the previous sections allow to understand the driving processes of sediment production and transport across the basin and the reasons for the reduction in SDR with variable erosion drivers. In this section we analyse how their balance determines the sediment load at the outlet.

In the distributed surface erodibility simulations (SIM 1 and 2) a reduced sediment yield (Y) is observed at the basin outlet and it is determined by a reduction in both sediment production (P) and sediment transport connectivity (SDR) with respect to uniform erodibility simulations (SIM 3 and 4):

$$\downarrow Y = SDR \downarrow \cdot P \downarrow . \tag{6}$$

In the distributed precipitation simulations (SIM 1 and 3) instead, an increased sediment yield at the basin outlet is observed compared to uniform precipitation simulations, this results from a combination of a smaller SDR and a much greater sediment production across the basin. The increase in sediment yield indicates that the greater sediment production dominates over the decreased sediment connectivity:

$$\uparrow Y = SDR \downarrow \cdot P \Uparrow . \tag{7}$$

This result means that the localized sediment source areas are triggered by the very high erosive power of localised precipitation captured by distributed simulations. Their signal reaches the outlet despite the system is globally less efficient in evacuating the eroded sediments. These hotspots of erosion are generated where precipitation falls with a high intensity, soil saturation is reached soon during storms, eventually favoured by shallow soils, and therefore hydrological and sediment flux connectivity are locally high.

In a hydrological modeling experiment conducted with TOPKAPI-ETH on the same catchment, Paschalis et al. (2014) demonstrated the dependence of the discharge peak on the clustering of high soil moisture areas. Our results show that the high soil moisture areas may also define the sediment signal. This finding also suggests that a large proportion of the sediment yield can be supplied by just few localized sediment sources (e.g. Pelletier, 2012). The role of soil moisture in producing high

https://doi.org/10.5194/esurf-2019-59
Preprint. Discussion started: 6 November 2019

sediment concentrations has also been highlighted by Dominic et al. (2015) and Brasington and Richards (2000), who attribute the peaks of SSCs to the connection of remote sediment sources during the wetting up of the catchment.

The relevance of soil moisture spatial distribution also explains why event sediment yields are more affected by the precipitation spatial variability, i.e. precipitation intensity, at low initial soil moisture than at high initial soil moisture (see Figure 9). This is due to the crucial role of precipitation intensity at low initial soil moisture in determining soil saturation and creating hydrological connectivity.

5 Conclusions

We presented a novel spatially distributed soil erosion and suspended sediment transport model based on the computationally efficient physically explicit hydrological model TOPKAPI-ETH. We showed that, by explicitly modelling hydrological processes, topographic and land cover effects on sediment transport in space and time, the model reproduces the creation of hotspots of sediment production, their catchment-wide connectivity, and thus the variability of sediment dynamics at the catchment scale.

Even if with a significant underestimation, when applied to a pre-alpine river basin, such a deterministic model reproduces a considerable part of the scatter of the observed SSC-Q relation, thus indicating that it contains some of the main temporal and spatial sources of concentration variability. The difference between observed and simulated SSC variability can be attributed to the contribution of localized threshold sediment sources and to the inherent randomness present in sediment production and transport at the catchment scale.

In this paper we used the model to investigate the role of spatial variability of erosion drivers on the spatial organization of suspended sediment transport. We consider precipitation and surface erodibility and observe that accounting for their spatial variability favors the simulation of clusters of sediment source areas and reproduces the effect of sediment buffer in reducing the connectivity of sediment sources to the river network. Sediment buffers in the case study basin are represented by topographically driven discontinuities in the south-eastern part of the basin and forests located around the river network across the whole basin. Accounting for the spatial variability of surface erodibility also reduces sediment production, which together with the reduced sediment transport connectivity determines a lower sediment yield at the outlet. The spatial distribution of precipitation has the effect to increase sediment production, which despite the reduced connectivity generates an increase in sediment yield, thus highlighting the key role of clusters of high soil moisture areas in defining the sediment signal.

Our results highlight the importance of resolving the spatial variations controlling the sediment production and transport processes to improve the predictive ability of model-based sediment dynamics assessments. A spatially distributed computationally efficient model like TOPKAPI-ETH integrated with a sediment module is be particularly suitable for applications at large scales, where gradients in climatic and physiographic characteristics control sediment production and transfer. Moreover, the type of analyses that we performed offer ways to investigate effects of future changes in rainfall intensity and patterns as well as scenarios of land use, which are expected to take place due to climate change or anthropic interventions. Future works

https://doi.org/10.5194/esurf-2019-59
Preprint. Discussion started: 6 November 2019

should look into the relation of localized sediment sources and mass wasting processes with spatial variability in precipitation and should focus on the effect of temporal changes of surface erodibility on concentration variability.

Data availability. DEM, soil and land use maps, discharge and suspended sediment concentrations data and simulation results are available at https://doi.org/10.3929/ethz-b-000358874. Meteorological input data can be requested at https://gate.meteoswiss.ch/idaweb/login.do.

Author contributions. GB developed the model, carried out the simulations and the analyses of the results. PM and PB contributed to the conceptualization of the model and to the discussion of the results. GB prepared the manuscript with contributions and edits from all co-authors.

Competing interests. The authors declare that they have no conflict of interest.

Acknowledgements. We thank Fritz Schlunegger for sharing his knowledge of the study basin. The study was funded by the DAFNE project, an Horizon 2020 programme WATER 2015 of the European Union, GA no. 690268.

https://doi.org/10.5194/esurf-2019-59
Preprint. Discussion started: 6 November 2019

References

Asselman, N. E.: Suspended sediment dynamics in a large drainage basin: The River Rhine, Hydrological Processes, 13, 1437–1450, https://doi.org/10.1002/(SICI)1099-1085(199907)13:10<1437::AID-HYP821>3.0.CO;2-J, 1999.

Asselman, N. E.: Fitting and interpretation of sediment rating curves, Journal of Hydrology, 234, 228–248, https://doi.org/10.1016/S0022-1694(00)00253-5, 2000.

Beasley, D. B., Huggins, L. F., and Monke, E. J.: ANSWERS: A Model for Watershed Planning, Transactions of the ASAE, 23, 0938–0944, https://doi.org/10.13031/2013.34692, http://elibrary.asabe.org/abstract.asp??JID=3&AID=34692&CID=t1980&v=23&i=4&T=1, 1980.

Bodeneignungskarte: 77.2 Digitale Bodeneignungskarte der Schweiz, https://www.blw.admin.ch/blw/de/home/politik/datenmanagement/geografisches-informationssystem-gis/download-geodaten.html, 2012.

Bracken, L. J., Turnbull, L., Wainwright, J., and Bogaart, P.: Sediment connectivity: A framework for understanding sediment transfer at multiple scales, Earth Surface Processes and Landforms, 40, 177–188, https://doi.org/10.1002/esp.3635, 2015.

Brasington, J. and Richards, K.: Turbidity and suspended sediment dynamics in small catchments in the Nepal Middle Hills, Hydrological Processes, 14, 2559–2574, https://doi.org/10.1002/1099-1085(20001015)14:14<2559::AID-HYP114>3.0.CO;2-E, 2000.

Chen, X. and Zong, Y.: Coastal Erosion Along the Changjiang Deltaic Shoreline, China: History and Prospective, Estuarine, Coastal and Shelf Science, 46, 733–742, https://doi.org/10.1006/ecss.1997.0327, https://linkinghub.elsevier.com/retrieve/pii/S0272771497903279, 1998.

Clapuyt, F., Vanacker, V., Schlunegger, F., Christl, M., and Van Oost, K.: Spatio-temporal dynamics of sediment transfer systems in landslide-prone alpine catchments, Solid Earth Discussions, pp. 1–22, https://doi.org/10.5194/se-2018-139, 2019.

CLC: Corine Land Cover (CLC) map 2012, https://land.copernicus.eu/pan-european/corine-land-cover/clc-2012, 2014.

Clinnick, P. F.: Buffer strip management in forest operations: A review, Australian Forestry, 48, 34–45, https://doi.org/10.1080/00049158.1985.10674421, 1985.

Collins, A. L. and Walling, D. E.: Progress in Physical Geography Documenting catchment suspended sediment sources : problems , approaches and prospects, Progress in Physical Geography, 2, 159–196, https://doi.org/10.1191/0309133304pp409ra, 2004.

Costa, A., Anghileri, D., and Molnar, P.: Hydroclimatic control on suspended sediment dynamics of a regulated Alpine catchment: A conceptual approach, Hydrology and Earth System Sciences, 22, 3421–3434, https://doi.org/10.5194/hess-22-3421-2018, 2018.

Coulthard, T. J., Neal, J. C., Bates, P. D., Ramirez, J., de Almeida, G. A., and Hancock, G. R.: Integrating the LISFLOOD-FP 2D hydrodynamic model with the CAESAR model: Implications for modelling landscape evolution, Earth Surface Processes and Landforms, 38, 1897–1906, https://doi.org/10.1002/esp.3478, 2013.

Davies-Colley, R. J. and Smith, D. G.: Turbidity, suspended sediment, and water clarity: A review, Journal of the American Water Resources Association, 37, 1085–1101, https://doi.org/10.1111/j.1752-1688.2001.tb03624.x, 2001.

Dominic, J. A., Aris, A. Z., and Sulaiman, W. N. A.: Factors Controlling the Suspended Sediment Yield During Rainfall Events of Dry and Wet Weather Conditions in A Tropical Urban Catchment, Water Resources Management, 29, 4519–4538, https://doi.org/10.1007/s11269-015-1073-0, 2015.

Dürst Stucki, M., Schlunegger, F., Christener, F., Otto, J. C., and Götz, J.: Deepening of inner gorges through subglacial meltwater - An example from the UNESCO Entlebuch area, Switzerland, Geomorphology, 139-140, 506–517, https://doi.org/10.1016/j.geomorph.2011.11.016, http://dx.doi.org/10.1016/j.geomorph.2011.11.016, 2012.

https://doi.org/10.5194/esurf-2019-59
Preprint. Discussion started: 6 November 2019

Duvert, C., Gratiot, N., Evrard, O., Navratil, O., Némery, J., Prat, C., and Esteves, M.: Drivers of erosion and suspended sediment transport in three headwater catchments of the Mexican Central Highlands, Geomorphology, 123, 243–256, https://doi.org/10.1016/j.geomorph.2010.07.016, http://dx.doi.org/10.1016/j.geomorph.2010.07.016, 2010.

Fatichi, S., Rimkus, S., Burlando, P., Bordoy, R., and Molnar, P.: High-resolution distributed analysis of climate and anthropogenic changes on the hydrology of an Alpine catchment, Journal of Hydrology, 525, 362–382, https://doi.org/10.1016/j.jhydrol.2015.03.036, http://dx.doi.org/10.1016/j.jhydrol.2015.03.036, 2015.

Ferguson, R. I.: River Loads Underestimated by Rating Curves, Water Resources Research, 22, 74–76, https://doi.org/10.1029/WR022i001p00074, 1986.

Francipane, A., Ivanov, V. Y., Noto, L. V., Istanbulluoglu, E., Arnone, E., and Bras, R. L.: TRIBS-Erosion: A parsimonious physically-based model for studying catchment hydro-geomorphic response, Catena, 92, 216–231, https://doi.org/10.1016/j.catena.2011.10.005, http://dx.doi.org/10.1016/j.catena.2011.10.005, 2012.

Frei, C. and Schär, C.: A precipitation climatology of the Alps from high-resolution rain-gauge observations, International Journal of Climatology, 18, 873–900, https://doi.org/10.1002/(SICI)1097-0088(19980630)18:8<873::AID-JOC255>3.0.CO;2-9, http://doi.wiley.com/10.1002/%28SICI%291097-0088%2819980630%2918%3A8%3C873%3A%3AAID-JOC255%3E3.0.CO%3B2-9, 1998.

Fryirs, K.: (Dis)Connectivity in catchment sediment cascades: A fresh look at the sediment delivery problem, Earth Surface Processes and Landforms, 38, 30–46, https://doi.org/10.1002/esp.3242, 2013.

Fryirs, K. and Brierley, G. J.: Slope – channel decoupling in Wolumla catchment , New South Wales, Australia : the changing nature of sediment sources following European settlement, Catena, 35, 41–63, https://doi.org/https://doi.org/10.1016/S0341-8162(98)00119-2, https://www.sciencedirect.com/science/article/pii/S0341816298001192, 1999.

Fryirs, K., Brierley, G. J., Preston, N. J., and Spencer, J.: Catchment-scale (dis)connectivity in sediment flux in the upper Hunter catchment, New South Wales, Australia, Geomorphology, 84, 297–316, https://doi.org/10.1016/j.geomorph.2006.01.044, 2007.

Fuller, C. W., Willett, S. D., Hovius, N., and Slingerland, R.: Erosion Rates for Taiwan Mountain Basins: New Determinations from Suspended Sediment Records and a Stochastic Model of Their Temporal Variation, The Journal of Geology, 111, 71–87, https://doi.org/10.1086/344665, 2003.

Gao, P.: Understanding watershed suspended sediment transport, Progress in Physical Geography, 32, 243–263, https://doi.org/10.1177/0309133308094849, 2008.

Hancock, G., Evans, K., Willgoose, G., Moliere, D., Saynor, M., and Loch, R.: Medium-term erosion simulation of an abandoned mine site using the SIBERIA landscape evolution model, Australian Journal of Soil Research, 38, 249–263, 2000.

Hancock, G. R., Webb, A. A., and Turner, L.: Sediment transport in forested head water catchments – Calibration and validation of a soil erosion and landscape evolution model, Journal of Hydrology, 554, 12–23, https://doi.org/10.1016/j.jhydrol.2017.08.049, http://dx.doi.org/10.1016/j.jhydrol.2017.08.049, 2017.

Hinderer, M., Kastowski, M., Kamelger, A., Bartolini, C., and Schlunegger, F.: River loads and modern denudation of the Alps - A review, Earth-Science Reviews, 118, 11–44, https://doi.org/10.1016/j.earscirev.2013.01.001, http://dx.doi.org/10.1016/j.earscirev.2013.01.001, 2013.

Horowitz, A. J.: An evaluation of sediment rating curves for estimating suspended sediment concentrations for subsequent flux calculations, Hydrological Processes, 17, 3387–3409, https://doi.org/10.1002/hyp.1299, 2003.

Kasten, F. and Czeplak, G.: Solar and terrestrial radiation dependent on the amount and type of cloud, Solar Energy, 24, 177–189, https://doi.org/10.1016/0038-092X(80)90391-6, 1980.

https://doi.org/10.5194/esurf-2019-59
Preprint. Discussion started: 6 November 2019

Kim, J., Ivanov, V. Y., and Fatichi, S.: Soil erosion assessment—Mind the gap, Geophysical Research Letters, 43, 12,446–12,456, https://doi.org/10.1002/2016GL071480, 2016.

Lang, A., Bork, H.-R., and Preston, N.: Changes in sediment flux and storage within a fluvial system : some examples from the Rhine catchment, Hydrological Processes, 3334, 3321–3334, https://doi.org/10.1002/hyp.1389, 2003.

Liu, Z. and Todini, E.: Towards a comprehensive physically-based rainfall-runoff model, Hydrology and Earth System Sciences, 6, 859–881, https://doi.org/10.5194/hess-6-859-2002, http://www.hydrol-earth-syst-sci.net/6/859/2002/, 2002.

Malmon, D. V., Dunne, T., and Reneau, S. L.: Stochastic Theory of Particle Trajectories through Alluvial Valley Floors, The Journal of Geology, 111, 525–542, https://doi.org/10.1086/376764, 2003.

Mekonnen, M., Keesstra, S. D., Stroosnijder, L., Baartman, J. E., and Maroulis, J.: Soil Conservation Through Sediment Trapping: A Review, Land Degradation and Development, 26, 544–556, https://doi.org/10.1002/ldr.2308, 2015.

Montgomery, D. R.: Soil erosion and agricultural sustainability, Proceedings of the National Academy of Sciences, 104, 13 268–13 272, https://doi.org/10.1073/pnas.0611508104, 2007.

Nearing, M. A., Foster, G. R., Lane, L. J., and Finkner, S. C.: A Process-Based Soil Erosion Model for USDA-Water Erosion Prediction Project Technology, Transactions of the ASAE, 32, 1587–1593, 1989.

Nearing, M. A., Pruski, F. F., and O'Neal, M. R.: Expected climate change impacts on soil erosion rates: A review, Journal of Soil and Water Conservation, 59, 43–50, 2004.

Norton, K. P., von Blanckenburg, F., Schlunegger, F., Schwab, M., and Kubik, P. W.: Cosmogenic nuclide-based investigation of spatial erosion and hillslope channel coupling in the transient foreland of the Swiss Alps, Geomorphology, 95, 474–486, https://doi.org/10.1016/j.geomorph.2007.07.013, 2008.

Olarieta, J. R., Besga, G., Rodríguez, R., Usón, A., Pinto, M., and Virgel, S.: Sediment enrichment ratios after mechanical site preparation for Pinus radiata plantation in the Basque Country, Geoderma, 93, 255–267, 1999.

Pappas, C., Fatichi, S., Rimkus, S., Burlando, P., and Huber, M. O.: The role of local-scale heterogeneities in terrestrial ecosystem modeling, Journal of Geophysical Research: Biogeosciences, 120, 341–360, https://doi.org/10.1002/2014JG002735, 2015.

Parkyn, S. M., Davies-Colley, R. J., Cooper, A. B., and Stroud, M. J.: Predictions of stream nutrient and sediment yield changes following restoration of forested riparian buffers, Ecological Engineering, 24, 551–558, https://doi.org/10.1016/j.ecoleng.2005.01.004, 2005.

Paschalis, A., Fatichi, S., Molnar, P., Rimkus, S., and Burlando, P.: On the effects of small scale space-time variability of rainfall on basin flood response, Journal of Hydrology, 514, 313–327, https://doi.org/10.1016/j.jhydrol.2014.04.014, http://dx.doi.org/10.1016/j.jhydrol.2014.04.014, 2014.

Pelletier, J. D.: A spatially distributed model for the long-term suspended sediment discharge and delivery ratio of drainage basins, Journal of Geophysical Research: Earth Surface, 117, 1–15, https://doi.org/10.1029/2011JF002129, 2012.

Pimentel, D., Allen, J., Beers, A., Guinand, L., Linder, R., McLaughlin, P., Meer, B., Musonda, D., Perdue, D., Poisson, S., Siebert, S., Stoner, K., Salazar, R., and Hawkins, A.: World Agriculture and Soil Erosion, BioScience, 37, 277–283, https://doi.org/10.2307/1310591, 1987.

Prosser, I. P. and Rustomji, P.: Sediment transport capacity relations for overland flow, Progress in Physical Geography, 24, 179–193, https://doi.org/10.1177/030913330002400202, http://journals.sagepub.com/doi/10.1177/030913330002400202, 2000.

Rickenmann, D., Badoux, A., and Hunzinger, L.: Significance of sediment transport processes during piedmont floods: The 2005 flood events in Switzerland, Earth Surface Processes and Landforms, 41, 224–230, https://doi.org/10.1002/esp.3835, 2016.

https://doi.org/10.5194/esurf-2019-59
Preprint. Discussion started: 6 November 2019

Schlunegger, F. and Schneider, H.: Relief-rejuvenation and topographic length scales in a fluvial drainage basin, Napf area, Central Switzerland, Geomorphology, 69, 102–117, https://doi.org/10.1016/j.geomorph.2004.12.008, 2005.

Schmidt, J. C. and Wilcock, P. R.: Metrics for assessing the downstream effects of dams, Water Resources Research, 44, https://doi.org/10.1029/2006WR005092, 2008.

Schmidt, S., Ballabio, C., Alewell, C., Panagos, P., and Meusburger, K.: Filling the European blank spot—Swiss soil erodibility assessment with topsoil samples, Journal of Plant Nutrition and Soil Science, 181, 737–748, https://doi.org/10.1002/jpln.201800128, 2018.

Schoonover, J. E., Williard, K. W. J., Zaczek, J. J., Mangun, J. C., and Carver, A. D.: Agricultural sediment reduction by giant cane and forest riparian buffers, Water, Air, and Soil Pollution, 169, 303–315, https://doi.org/10.1007/s11270-006-3111-2, 2006.

Schwab, M., Rieke-Zapp, D., Schneider, H., Liniger, M., and Schlunegger, F.: Landsliding and sediment flux in the Central Swiss Alps: A photogrammetric study of the Schimbrig landslide, Entlebuch, Geomorphology, 97, 392–406, https://doi.org/10.1016/j.geomorph.2007.08.019, 2008.

Schwarb, M.: The alpine precipitation climate evaluation of a high-resolution analysis scheme using comprehensive rain-gauge data, ETH Zurich Research Collection, https://doi.org/10.3929/ethz-a-010782581, 2000.

Seeger, M., Errea, M. P., Beguería, S., Arnáez, J., Martí, C., and García-Ruiz, J. M.: Catchment soil moisture and rainfall characteristics as determinant factors for discharge/suspended sediment hysteretic loops in a small headwater catchment in the Spanish pyrenees, Journal of Hydrology, 288, 299–311, https://doi.org/10.1016/j.jhydrol.2003.10.012, 2004.

Siakeu, J., Oguchi, T., Aoki, T., Esaki, Y., and Jarvie, H. P.: Change in riverine suspended sediment concentration in central Japan in response to late 20th century human activities, Catena, 55, 231–254, https://doi.org/10.1016/S0341-8162(03)00120-6, 2004.

Smith, B. P., Naden, P. S., Leeks, G. J., and Wass, P. D.: The influence of storm events on fine sediment transport, erosion and deposition within a reach of the River Swale, Yorkshire, UK, Science of the Total Environment, 314-316, 451–474, https://doi.org/10.1016/S0048-9697(03)00068-8, 2003.

SwissAlti3D: SwissAlti3D - The high precision digital elevation model of Switzerland, https://shop.swisstopo.admin.ch/en/products/height_models/alti3D, 2017.

Syvitski, J. and Kettner, A.: Sediment flux and the anthropocene, Philosophical Transactions of the Royal Society A: Mathematical, Physical and Engineering Sciences, 369, 957–975, https://doi.org/10.1098/rsta.2010.0329, 2011.

Syvitski, J., Vörösmarty, C. J., Kettner, A. J., and Green, P.: Impact of Humans on the Flux of Terrestrial Sediment to the Global Coastal Ocean, Science, 308, 376–380, https://doi.org/10.1126/science.1109454, http://www.sciencemag.org/cgi/doi/10.1126/science.1109454, 2005.

Tsuruta, K., Hassan, M. A., Donner, S. D., and Alila, Y.: Development and Application of a Large-Scale, Physically Based, Distributed Suspended Sediment Transport Model on the Fraser River Basin, British Columbia, Canada, Journal of Geophysical Research: Earth Surface, 123, 2481–2508, https://doi.org/10.1029/2017JF004578, 2018.

Van Den Berg, F., Schlunegger, F., Akçar, N., and Kubik, P.: 10Be-derived assessment of accelerated erosion in a glacially conditioned inner gorge, Entlebuch, Central Alps of Switzerland, Earth Surface Processes and Landforms, 37, 1176–1188, https://doi.org/10.1002/esp.3237, 2012.

Van Rompaey, A. J., Verstraeten, G., Van Oost, K., Govers, G., and Poesen, J.: Modelling mean annual sediment yield using a distributed approach, Earth Surface Processes and Landforms, 26, 1221–1236, https://doi.org/10.1002/esp.275, 2001.

https://doi.org/10.5194/esurf-2019-59
Preprint. Discussion started: 6 November 2019

555 Vercruysse, K., Grabowski, R. C., and Rickson, R. J.: Suspended sediment transport dynamics in rivers: Multi-scale drivers of temporal variation, Earth-Science Reviews, 166, 38–52, https://doi.org/10.1016/j.earscirev.2016.12.016, http://dx.doi.org/10.1016/j.earscirev.2016.12.016, 2017.

Walling, D. E.: Assessing the accuracy of suspended sediment rating curves for a small basin, Water Resources Research, 13, 531–538, https://doi.org/10.1029/WR013i003p00531, 1977.

560 Walling, D. E.: The sediment delivery problem, Journal of Hydrology, 65, 209–237, https://doi.org/10.1016/0022-1694(83)90217-2, 1983.

Walling, D. E.: Human impact on land-ocean sediment transfer by the world's rivers, Geomorphology, 79, 192–216, https://doi.org/10.1016/j.geomorph.2006.06.019, 2006.

Walling, D. E. and Webb, B. W.: The reliability of suspended sediment load data, Journal of the American Medical Association, 248, 2180, https://doi.org/10.1001/jama.248.17.2180, 1982.

565 Wass, P. D. and Leeks, G. J. L.: Suspended sediment Fluxes in the Humber catchment , UK, Hydrological Processes, 953, 1999.

Wittmann, H., von Blanckenburg, F., Kruesmann, T., Norton, K. P., and Kubik, P. W.: Relation between rock uplift and denudation from cosmogenic nuclides in river sediment in the Central Alps of Switzerland, Journal of Geophysical Research: Earth Surface, 112, 1–20, https://doi.org/10.1029/2006JF000729, 2007.

Woolhiser, D., Smith, R. E., and Goodrich, D.: A Kinematic Runoff and Erosion Model, 1990.

570 Yang, D., Kanae, S., Oki, T., Koike, T., and Musiake, K.: Global potential soil erosion with reference to land use and climate changes, Hydrological Processes, 17, 2913–2928, https://doi.org/10.1002/hyp.1441, 2003.

Zabaleta, A., Martínez, M., Uriarte, J. A., and Antigüedad, I.: Factors controlling suspended sediment yield during runoff events in small headwater catchments of the Basque Country, Catena, 71, 179–190, https://doi.org/10.1016/j.catena.2006.06.007, 2007.